LBL--11669

DE82 018932

LBL-11669

MAGNETIC FIELD, CLOSED ORBIT, AND ENERGY MEASUREMENT IN THE BEVATRON

Kenneth C. Crebbin

Accelerator and Fusion Research Division
Lawrence Berkeley Laboratory
University of California
Berkeley, California 94720

November 1981

DISCLAIMER

This work was supported by the Director, Office of Energy Research, Office of High Energy and Nuclear Physics, Division of High Energy Physics of the U.S. Department of Energy under Contract Number DE-AC03-76SF00098.

MAGNETIC FIELD, CLOSED ORBIT, AND ENERGY MEASUREMENT IN THE BEVATRON

Kenneth C. Crebbin

This report provides the information necessary for a better evaluation of particle energy in the Bevatron. Previously, the nominal magnetic field value and radius were used to calculate the value for the kinetic energy of the particle. This value was good to a few percent. Today, more and more experimenters would like to know the energy to a more precise value. To this end, corrections to the measured magnetic field values and the radial closed orbit are provided.

I. BEVATRON MAGNETIC FIELD

A. Basic Field Shape

The radial field shape of the Bevatron is described by:

$$B = B_o R_o^n / R^n \quad , \tag{1-1}$$

where: B is the field value at radius R;

B_o is the field value at radius R_o; and

n is the field index.

Whenever a field value is specified for Bevatron operation, it is the value B_o, which is the value at a radius of 599.375 inches. The magnetic field value used to calculate the energy of the particle is then given by Eq. (1-1) for the specific operating radius of the beam. Details of the calculations are given in another report.[1] There are tables of the results in the MCR of the Bevatron, and there is a computer program, PAM, in the MODCOMP that can be used to calculate values for each specific case.

B. Monitoring of Magnetic Field

The original magnetic field measurements were done in 1953-1954. The results are summarized in an engineering note.[2] The magnetic field values as originally measured are referenced to what is called an I-pip. The I-pip system is a set of pulses that are generated from a current transformer on the main conductors to the Bevatron magnet windings. Each I-pip pulse corresponds to a specific current in the main Bevatron coil windings. This current is then related to a specific field value as measured in 1953-1954. This is the primary standard for field measurements in the Bevatron.

The Bevatron main field windings are bi-filar. There are therefore two I-pip systems, called the East system and the West system. East-West is the location of the current transformers in the shunt house and does not indicate current in the East or West half of the Bevatron magnet. Both sets of winding go through all four quadrants in series.

There are three sets of windings on the face of the pole tips. There is a set of 21 windings at 3-inch spacing radially across the aperture. These are called pole face windings (PFW) and are used to shape the Bevatron guide field by changing the field index n [Eq. (1-1)]. Windings number 1 and 21 were in the stanchions. These were removed in 1962. The remaining windings are numbered 2 through 20. Winding number 11 is on the gap centerline at a radius of 599.375 inches. Parallel to PFW 2 and 20 are two additional windings used to control ripple in the main guide field during beam spill. These are called ripple reduction windings.

Midway between PFW 6, 7, and 8 and PFW 14, 15, and 16 are two sets of windings called B-dot windings. The winding between PFW 6 and 7 crosses over at the end of the quadrant and returns between PFW 14 and 15. This forms a

loop around the center 21 inches (radially) of each quadrant. This loop is used to measure the change of magnetic flux in that part of the aperture. Similarly, the winding between PFW 7 and 8 returns between PFW 15 and 16. There are four sets of loops, two on the lower pole tips and two on the upper pole tips. The loops can be wired in series to provide a complete loop around the Bevatron or brought out on a quadrant-by-quadrant basis.

The voltage across this coil from the rate of change of magnetic flux within the loop can be integrated to provide a signal that is proportional to the dynamic magnetic field. This is called the B-dot integrator. The output from a B-dot integrator has been used since 1962 to program the rf oscillator during particle acceleration in the Bevatron. In 1969, the output from a B-dot integrator was used to provide a set of marker pulses at each kilogauss level of magnetic field in the Bevatron. These pulses were distributed to the operations and experimental groups at the Bevatron in place of the old I-pip system. Special pulses can be provided from the system in steps of 0.01 gauss. A digital readout is provided to monitor the value of the magnetic field on a flat top.

Because the value from the B-dot integrator is proportional to the dynamic field, there are several problems. The value does not include the remnant field in the Bevatron, which is typically between 35 and 40 gauss. It also has to be calibrated to read the correct value of the field. In addition, the radial shape of the field changes as the pole tips saturate at high field. Therefore, the integrated value from the B-dot loop does not have a constant relationship to the value at gap centerline.

The remnant-field value can be provided in two ways: a constant value is simply added into the starting value of the B-dot integrator; or a remnant-field magnetometer can be used to dynamically read the remnant field and provide that value as a starting point for the B-dot integrator. At present, the former method is normally used.

The basic calibration was done by setting the remnant-field value at the start of the Bevatron pulse and then adjusting the B-dot integral value to read the tabulated value for B-field at some I-pip. In 1975, the I-pip chosen was I-27. However, in a recheck of calibration in June 1977, the calibration was changed to give the tabulated field value at I-26. The reason for making this change and the consequences of the change will be discussed later, after some of the field variations are examined.

C. Variations in Magnetic Field

In the early days of proton running at the Bevatron, the values for the particle energy were taken as a function of I-pip from Engineering Print 9Y7083A.[3] Extrapolation in time between I-pips was done in the table to determine particle energy. When the B-dot integrator system was installed, the calibration was done using the tabulated values for B-field and I-pips in the above print. The energy was then calculated using the value of the B-field read by the B-dot integrator.

The original Bevatron magnetic field measurements are summarized in Engineering Note UCID-599 (MT-87).[2] In using this note's azimuthal variation of magnetic field, as given on page BFS-20, to calculate the radial closed orbit, I noted that there were no values plotted for the entrance

and exit sectors of each quadrant. I discussed this with Glen Lambertson, and he said the values for those sectors were included in a table giving the effective length of each quadrant. These measurements were made using a long coil covering the end sector and well into the straight section. These values are given on page PFS-4 of MT-87.[2]

There are two things of interest in this table: the increase in effective field length of the quadrant causes a substantial shift in the closed orbit (over 13 inches); and the tabulated values of magnetic field as a function of I-pip are different from the values tabulated in 9Y7083A. In fact, the values in 9Y7083A are tabulated as "effective flux density at marker." In MT-87, the values are tabulated as "average total flux density."

From discussion of this with Glen Lambertson, it appears that the field and energy values tabulated in 9Y7083A were corrected for the effective quadrant length. The magnetic field values tabulated are the effective field that would exist in a 90-degree quadrant to give the correct energy consistent with the shifted closed orbit. The magnetic field that one would measure at some sector at any I-pip are those values tabulated in MT-87 page BFS-4. The values in both reports are listed in Table 1. The effect on the closed orbit and particle energy will be discussed later. First, I will examine in more detail the calibration of the B-dot integrator, in light of this information on tabulated values for magnetic field as a function of I-pip.

The B-dot integrator calibration in May 1975 is reported in a memorandum dated June 24, 1975.[3] The values of B from the B-dot integrator are tabulated in Table 1, along with the values of B from 9Y7083A and MT-87. A plot of the differences for the values for the B-dot integrator and 9Y7083A is

Table 1. Comparison of two calibrations of magnetic field values as a function of I-pip. Sources: Refs. 2 and 3.

I-pip	BA	BB	QL	1975 Calibration $\int\dot{B}$	1975 Calibration ΔBA	1975 Calibration ΔBB	1977 Calibration $\int\dot{B}$	1977 Calibration ΔBA	1977 Calibration ΔBB	1975 $\frac{\Delta BA}{BA}$	1977 $\frac{\Delta BA}{BA}$	1977 $\frac{\Delta BB}{B}$
	Gauss	Gauss	Inches	Gauss	Gauss	Gauss	Gauss	Gauss	Gauss	$\times 10^{-3}$	$\times 10^{-3}$	$\times 10^{-3}$
I-10	1019	1007	7.0	1017	-2	+10	1018	-1	+11	-1.96	-0.98	+11.0
I-15	1727	1713	7.6	1708	-19	-5	1712	-15	-1	-11.0	-8.7	-0.58
I-20	3184	3193	7.8	3198	+14	+5	3206	+22	+13	+4.4	+6.9	+4.1
I-21	3832	3820	7.6	3810	-22	-10	3820	-12	0	-5.7	-3.1	0
I-22	4833	4859	7.5	4849	+16	-10	4862	+29	+3	+3.3	+6.0	+0.62
I-23	6083	6130	6.9	6088	+5	-42	6104	+21	-26	+0.82	+3.5	-4.2
I-24	7554	7599	5.2	7561	+7	-38	7582	+28	-17	+0.93	+3.7	-2.2
I-25	8890	8921	2.9	8894	+4	-27	8916	+26	-5	+0.45	+2.9	-0.56
I-26	10948	10954	0.3	10927	-21	-27	10954	+6	0	-1.9	+0.55	0
I-27	12428	12425	-0.5	12426	-2	+1	12455	+27	+30	-0.16	+2.2	+2.4

BA = Field values from MT-87.
BB = Field values from 9Y7083A.

shown in Fig. 1a. The calibration point here was I-27, with a dynamic reading for residual field added into the value from the B-dot integrator.

In June 1977, another calibration was done. At that time, the calibration was shifted to I-26 to provide a better fit to the values tabulated in 9Y7083A. The values from the B-dot integrator for this calibration are also shown in Table 1 and plotted in Fig. 1b. This was an unfortunate change, as it lowered the Bevatron field by 27 gauss at I-26 with a corresponding decrease in kinetic energy of the particles. In addition, the value for B at I-26 seems to be one of several original measurements that are in error. This will be shown in the following analysis.

The values for B from the B-dot integrator are replotted as $(B_{int}-B)/B$, where B is the value given at each I-pip from 9Y7083A. This is shown in Fig. 2a; Fig. 2b is the same curve using the values of B given in MT-87. Compare these curves to the calculated curve for $\Delta B/B$. The calculated curves were determined by computing the value of B enclosed by the B-dot loop relative to the central value of B at a radius of 599.375 inches using the radial field plots of B in MT-87. This the curve plotted as Fig. 2c. The B-dot loop connected to the B-dot integrator is on the lower pole tips between PFW 7 and 8, and returns between PFW 15 and 16.

A second correction was made by assuming that all the additional flux from the effective quadrant length change was included in the B-dot loop. This correction is added to the above radial calculation (Fig. 2c) to give the calculated curve for the B-dot integrator curve Fig. 2d.

In Fig. 1a and Fig. 2a, we see that the B-dot integrator gave a value for B lower than those tabulated in 9Y7083A for lower values than the calibration value. This was the reason for the change in calibration point in 1977--to

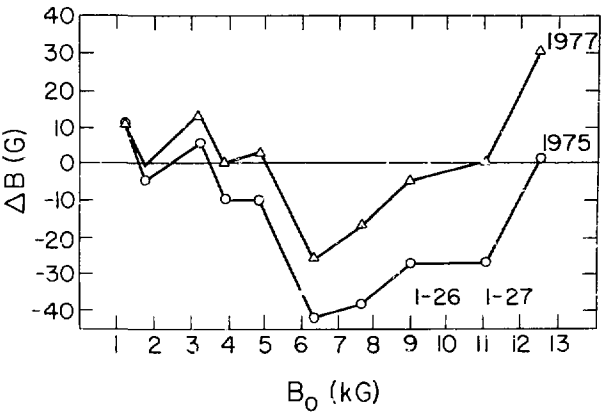

XBL 824-434

Fig. 1. $\Delta B = \int \dot{B} - B$, where B is the values tabulated in 9Y7083A.

(a) o 1975 calibration, $\Delta B = 0$ at I-27.

(b) Δ 1977 calibration, $\Delta B = 0$ at I-26.

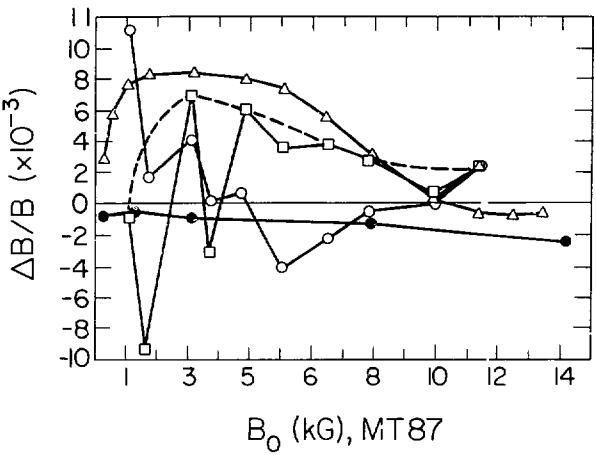

X3L 824-429

Fig. 2. Plot of $\Delta B/B$ vs values of B_0

(a) ○ 1977 data $\Delta B = \int \dot{B}$-B values from 9Y7083A.

(b) □ 1977 data $\Delta B = \int \dot{B}$-B values from MT-87.

(c) ● ΔB = B(calc)-B(MT-87)B(calc) from radial shape integrated over radial area of B dot loop, normalized to field at R_0 = 599 3/8 inches.

(d) △ ΔB = B(calc)-B(MT-87)B(calc) from c above plus magnetic field from quadrant length extension assuming all the flux is contained within the B-dot loop.

get a better fit, as shown in Fig. 1b. Note that below 6,000 gauss the values do not follow any smooth curve. If we look at graph 2b, where the field values given in MT-87 are used, we see a more reasonable fit to calculated curve 2d. Note that the value at 10,948 gauss, chosen as the 1977 calibration reference, is below the smooth curve and appears to be an incorrect measurement in the original field calibrations. There are also a few variations in the lower field values at 3,832 gauss and at 1,727 gauss. If one put ±0.3% error bars on these values, most of the points would fall within this range.

The conclusions to be drawn from these graphs are that the original basic field measurements are not accurate enough for precise particle energy measurements. Also, the B-dot coil in the Bevatron does not measure the field at gap centerline. In addition, the amount of flux integrated relative to the flux at gap centerline changes as a function of field so that no simple calibration at one value of B can be scaled to another field value with the accuracy desired by some experimenters. In general, the particle energy determined by the field value from the B-dot integrator and the particle radius is good only to a few percent.

A more accurate value can be calculated by making the appropriate field corrections, using the curves of Fig. 2b to determine the value for B. An additional correction for the extra quadrant lengths must be made. This can be as much as a 1.5% correction in the value of the kinetic energy. From Fig. 2b and 2d, it is apparent that part of the fringe field is included in the integral value of B, so that a complete orbit correction, as given in Section II-B, will be an overcorrection.

II. CLOSED ORBIT

A. Calculations for Normal Azimuthal Variation of Magnetic Field

There are several reasons for wanting to know the closed orbit of a particle in the Bevatron. The one we are concerned with is to determine the path length. Then, knowing the time it takes to go once around the Bevatron, we can determine the kinetic energy of the particle by time of flight. Any closed orbit can be described by Fourier analysis in the form:

$$R = R_0 + \Sigma \left[a(i)\cos(i\theta) + b(i)\sin(i\theta)\right] \quad . \tag{2-1}$$

A detailed report on the harmonic analysis of the vertical closed orbit is given in a Bevatron report.[5] It needs only a minor change to use it to calculate the radial closed orbit.

I have a computer program that calculates the closed orbit by averaging a general betatron oscillation over many turns. It gives essentially the same results as the harmonic analysis calculation and is simpler to use.

Let us now see what we can determine about the path length of the particle around the Bevatron without knowing the exact closed orbit at each sector in the Bevatron. From Eq. (2-1), we see that the closed orbit can be represented by a series of sinusoidal oscillations, all an integral multiple of 2π once around the Bevatron.

Let us now examine the path length of a sinusoidal oscillation around a uniform orbit.

$$R = R_0 + a\sin(i\theta) \quad ,$$

$$d\ell = R d\theta \quad , \tag{2-2}$$

$$\int d\ell = \int_0^{2\pi/i} R d\theta = \int_0^{2\pi/i} (R_0 + a\sin(i\theta))\, d\theta \quad ,$$

$$L = (2\pi/i)R_0 \text{ for a single oscillation around the closed orbit.}$$

The extra path length traveled by the sinusoidal oscillation just cancels, and the path length is equal to the fixed orbit path length $R_0\theta$. In Eq. (2-1), we can see that the harmonic parts average out to zero in each cycle of oscillation, and the path length is just equal to $2\pi R_0$ plus the straight sections.

At the Bevatron, the closed orbit is measured using radial probes. A U-shaped target is flipped up into the beam. The target is adjusted radially to give maximum beam survival. The center of the U target is at the center of the beam. This is repeated at each target position. We have target positions in each straight section, so we have four measurements 90 degrees apart.

Substituting in Eq. (2-1) for J measurements and summing, we have:

$$\sum_{j=1}^{n} R_j = nR_0 + \sum_{j=1}^{n} a(i)\cos(i\theta_\omega) + \sum_{j=1}^{n} b(i)\sin[i\theta(J)] \quad .$$

This reduces to:

$$\sum_{j=1}^{n} R_j = nR_0 + n(a(n) + a(2n) + a(3n) \ldots) \quad ,$$

$$R_0 = \frac{1}{n} \sum_{j=1}^{n} R_j - [a(n) + a(2n) + a(3n) \ldots] \quad . \tag{2-3}$$

That is, we know the value for R_0 to within the error of the amplitude of the nth + 2nth + . . . harmonic for n azimuthally equidistant measurements of radial position. For measurements at each straight section, the error in the measured value for R_0 is the amplitude of the 4th, 8th, 12th . . . harmonic. The question is, can we put an upper limit on the amplitude of these harmonic oscillations without knowing the exact closed orbit?

An upper limit can be calculated for the case of a systematic fourth-order perturbation in the field value of each sector. The coefficients for the ith harmonic are derived by substituting Eq. (2-1) into the second-order differential equation for radial betatron oscillations. This yields:

$$\begin{matrix} a_i \\ b_i \end{matrix} = \frac{k^2(1-n)}{k^2(1-n) - i^2} \frac{1}{\pi_0} \int_0^{2\pi} A(j) \begin{matrix} \cos(i\theta) \\ \sin(i\theta) \end{matrix} ,$$

where: $k = 1 + 4L/2\pi R = 1.$ [illegible],

L = length of straight sections,

R = radius of curved sections,

$A(j)$ = shift in equilibrium orbit position from the reference orbit position, in the jth sector, for a change in magnetic field value in the jth sector from the nominal value.

The integral is over both curved and straight sections. As we are interested in the approximate value of a fourth harmonic, we can ignore the slight correction contributed by integrating over the straight section. The major correction to amplitudes from the straight section is included in the k term.

Set A equal to 18 inches (1% perturbation) for each sector, with a sign change always additive for the sin iθ term. The cosine term then sums to zero.

$$b(4) = \frac{k^2(1-n)}{k^2(1-n)-16} \frac{1}{\pi} A_o \; 8 \int_0^{\pi/4} \sin 4\theta \, d\theta$$

$$= \frac{k^2(1-n)}{k^2(1-n)-16} \frac{8}{\pi} A_o \left[\frac{-\cos 4\theta}{4}\right]_0^{\pi/4}$$

$$= \frac{k^2(1-n)}{k^2(1-n)-16} \frac{8}{\pi} A_o \frac{1}{2} \; .$$

Substituting for $k = 1.255$, $n = 0.66$, $A_o = 18$,

$$b(4) = \frac{(1.255)^2 \, (0.34)}{(1.255)^2 \, (0.34) - 16} \frac{4 \times 18}{\pi}$$

$$= \frac{0.536}{0.536 - 16} \times \frac{4 \times 18}{\pi}$$

$$= 0.035 \times \frac{4 \times 18}{\pi}$$

$$b(4) = 0.794 \text{ inches.}$$

A highly systematic perturbation of 1% at each sector of the Bevatron thus produces a closed orbit distortion of only 0.8 inches.

Another way of examining the fourth-harmonic problem is to consider the Bevatron as being made up of 144 perfect sectors plus 144 local perturbations centered at each sector. The variation of the magnetic field at each sector can be considered as a radial bend or kick localized azimuthally at a point. For a perfect machine, we know what the orbit is with such a localized radial kick; we have simply a sin νθ curve which closes at the perturbation, has a

maximum radial displacement 180 degrees from the perturbation, and is symmetric about the point 190 degrees from the perturbation. This is shown in Figs. 3 and 4. The closed orbit is then the sum of the 144 terms.

The detailed derivation is given in the Appendix. There, the closed orbit is given by Eq. (A-5):

$$R(i) = A(i) \cos\left[\nu\theta(i) + D(i)\right] \tag{2-4}$$

where A(i) and D(i) are slowly varying functions. The basic closed orbit is therefore a distorted first harmonic.

The change in R from phase shift and amplitude changes due to the perturbation is given by Eq. (A-11) in the Appendix:

$$\Delta R(i,i+1) = 2A(i) \sin(\nu\pi)\, \nu\Delta\theta \quad . \tag{2-5}$$

To evaluate A(i) for a perturbation of 1%, we proceed as follows. Consider Eq. (2-4) describing a single perturbation path so that A and D are constants. The perturbation will be just 2 times the $dR/d\theta$ at the perturbation.

$$\text{At } \theta = 0, \quad R = -A(i) \quad ,$$

$$-A(i) = A(i) \cos(\nu 0 + D), \text{ therefore } D = \pi \quad ;$$

$$R = A(i) \cos(\nu\theta + \pi) \quad ,$$

$$\frac{dR}{d\theta} = -A(i)\, \nu \sin(\nu\theta + \pi) \quad ,$$

$$\frac{dR}{d\theta} = -A(i)\, \nu \sin(\nu\pi + \pi)$$

$$= -A(i)\, \nu \sin(\nu\pi) \cos(\pi) + \cos(\nu\pi) \sin(\pi) \quad ,$$

$$\frac{1}{\nu}\frac{dR}{d\theta} = A(i) \sin(\nu\pi)$$

$$P = 2\frac{dR}{dS} = 2\frac{dR}{R\,d\theta} = \frac{2\nu}{R}\frac{1}{\nu}\frac{dR}{d\theta} \quad .$$

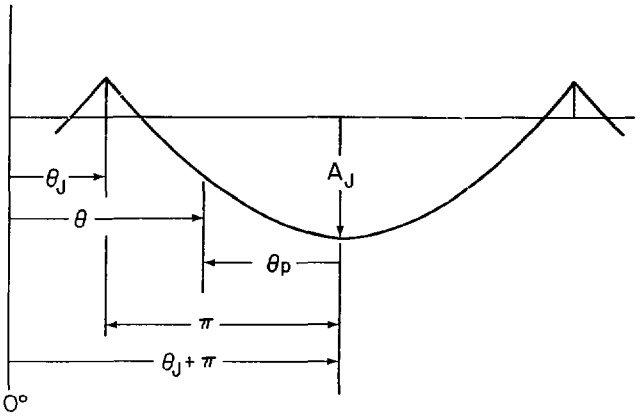

XBL 824 438

Fig. 3. Closed orbit through perfect machine with perturbation at θ_j, for case $\theta > \theta_j$.

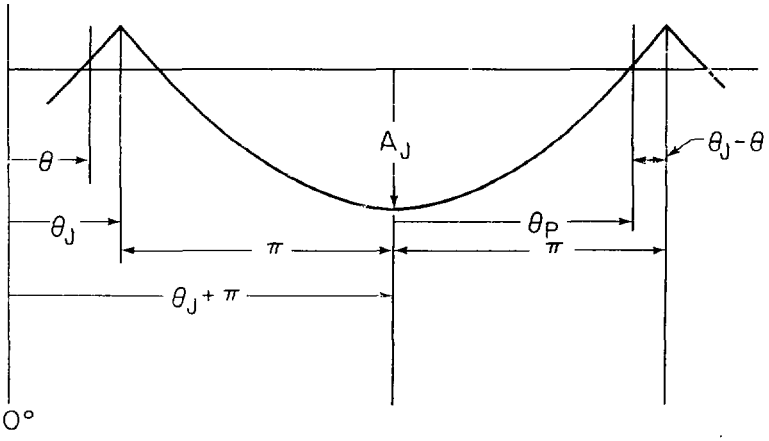

XBL 824-437

Fig. 4. Closed orbit through perfect machine with perturbation at θ_j, for case $\theta < \theta_j$.

For a 1% perturbation,

$$P = 0.01\Delta\theta \quad ,$$

where: $\Delta\theta = 2.5°$ (angular bend of one sector),

$$0.01\ \Delta\theta = \frac{2\nu}{R}\frac{1}{\nu}\frac{dR}{d\theta}$$

$$= \frac{2\nu}{R}\left[A(i)\ \sin\ (\nu\pi)\right] \quad ,$$

$$A(i) = \frac{0.01\ \Delta\theta R}{2\ \nu\ \sin\ (\nu\pi)} \quad .$$

Substitute in Eq. (2-5), for R = 604 inches; $\nu = 0.667$;

$$\Delta R(i,i+1) = 2\ \frac{0.01\ \Delta\theta R}{2\ \nu\ \sin\ (\nu\pi)}\ \sin\ (\nu\pi)\nu\Delta\theta$$

$$= 0.01\ R(\Delta\theta)^2$$

$$\Delta R(i,i+1) = 1.15 \times 10^{-2} \text{ inches/sector} \quad .$$

Besides this change in R from the local perturbation, there is the change in R due to the change in θ for a constant amplitude and phase. This is given by:

$$R = A\ \sin\ (\nu\theta + D) \quad ,$$

$$dR = A\nu\ \cos\ (\nu\theta + D)\ d\theta \quad ,$$

The maximum value for this is:

$$dR_m = A \times 0.667 \times 1 \times \frac{2.5^{\circ}}{180}\ \pi \quad ,$$

$$dR_m = A \times 0.029 \quad .$$

For a 1-inch amplitude of first harmonic distortion,

$$dR = 0.029 \text{ inches per sector.}$$

For a 2-inch amplitude,

$$dR_m = 0.058 \text{ inches per sector.}$$

A fourth harmonic oscillation covers nine sectors; therefore, for the case of the 2-inch first harmonic amplitude plus the change in R per sector from the perturbation, the maximum displacement is:

$$\Delta R = [0.058 + 0.115] \times 9 \quad ,$$

$$\Delta R = 0.63 \text{ inches} \quad .$$

This is about the same value as calculated for a systematic fourth harmonic around the entire machine using harmonic analysis.

Both of these analyses assume a very systematic perturbation. If 20% of this perturbation is undetected in our closed orbit measurements, we would have an uncertainty in R_0 of ±0.16 inches from the undetected fourth-order harmonic.

Closed orbit measurements at the four straight sections give a good estimate of the average value of the closed orbit R_0 without our having to know the actual path of the closed orbit for normal sector perturbations.

B. Variation of Effective Quadrant Length

As mentioned earlier, the major perturbation to the closed orbit is from the variation of the magnetic field involved in the change in effective length of the quadrants. The easiest method of studying particle trajectories is with the concept of betatron oscillations. Implicit in the derivation is the assumption that the particles are bent through an angle of 2π in following the closed orbit. If the effective magnetic field length is less or greater than 2π, then the difference must be handled as a perturbation superimposed on a normal betatron path.

For a perturbation that is the same for each quadrant, this orbit is a section of betatron oscillation symmetric about the center of each quadrant. The extra bend at the end of the quadrant is considered a localized perturbation just equal to the derivative of the betatron oscillation at that point (see Fig. 5). If the quadrant is longer than 90 degrees, the deflection is radially inward. If the quadrant is less than 90 degrees, the deflection is radially outward.

The displacement r is given by;

$$r = A \sin(\sqrt{1-n} + \theta + D) \quad ; \tag{2-6}$$

at $\theta = 0, \quad r = -A(1)$,

$$-A(1) = A \sin(D).$$

Therefore:

$$D = \frac{3\pi}{2} \quad ; \quad A = A(1) \quad ,$$

$$r = A(1) \sin\left(\sqrt{1-n}\,\theta + \frac{3\pi}{2}\right) = -A(1) \cos \sqrt{1-n}\,\theta \quad ,$$

$$R = R_E - r \quad ,$$

$$R = R_E + A(1) \cos(\sqrt{1-n}\,\theta) \quad .$$

For $n = 0.688$, $\sqrt{1-n} = \sqrt{1-0.668} = 0.576$.

The perturbation $\alpha = DL/R = dR/ds$; therefore:

$$\frac{dR}{d\theta} = \frac{R}{I}\frac{dR}{ds} = -0.056\, A(1) \sin(0.576\, \pi/4) \quad \text{at the perturbation,}$$

$$R\frac{DL}{R} = -0.576\, A(1) \sin(0.576\, \pi/4) \quad ,$$

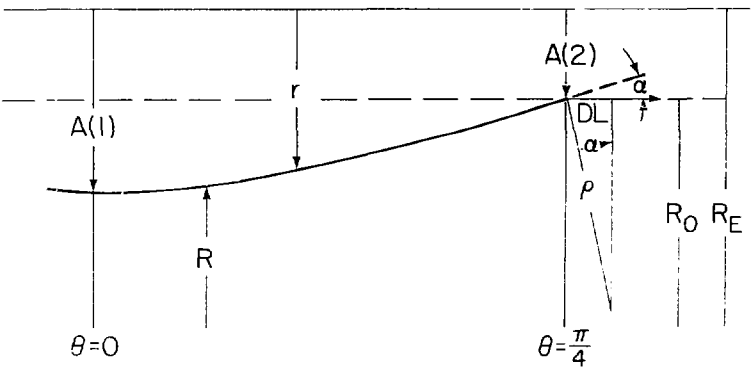

XBL 824-435

Fig. 5. R_E is the radius for the energy of the particle for a normal magnetic field. R_o is the reference closed orbit at the straight section with end perturbation DL to just remove α at the straight section. A(2) is the amplitude of the betatron oscillation at the straight section relative to R_E. A(1) is the maximum amplitude of the betatron oscillation at the center of the quadrant relative to R_E.

$$A(1) = \frac{-DL}{0.576 \sin (0.576\ \pi/4)} ,$$

$$A(1) = -3.969\ DL ,$$

$$A(2) = r = -A(1) \cos (0.576\ \pi/4) ,$$

$$A(2) = -3.9692\ DL \cos (0.576\ \pi/4) ,$$

$$A(2) = -3.57\ DL . \qquad (2\text{-}7)$$

For a quadrant increase of 7.5 inches, DL = 7.5/2 = 3.75 inches. Therefore, A(2) = -13.39-inch displacement of the closed orbit at the straight section.

At the center of the quadrant, the orbit is shifted

$$A(1) = -3.97 \times 3.75 = -14.9 \text{ inches.}$$

This is a substantial shift, equal to a change of about 1.3% in en .gy at 400 MeV/amu.

At high field, the quadrants are less than 90 degrees. The effect is the same, but the orbit is moved outward. At a 12.5 kG field, DL is 0.5/2 = 0.25 inches.

The scallop in the quadrant is just the difference between A(1) and A(2) above:

$$\Delta A = -(3.97 - 3.57)\ DL ,$$

$$\Delta A = -0.40\ DL.$$

For the high field case, this is:

$$\Delta A = -0.40 \times (-0.25) = +0.1 \text{ inches} .$$

The measured difference is about 0.5 inches, as shown in a plot of closed orbit through quadrant III measured in 1968 during resonant extraction studies (Fig. 6). This was done using the travel through target. This 0.5-inch offset was measured from a straight-line extrapolation between the West and North straight sections. There is an obvious closed-orbit distortion in addition to the scallop shown in the measurements. If a calculated closed orbit that approximates the position in the North and West is examined, the offset is about 0.25 inches. A complete closed-orbit measurement at high field is not at present available.

Graphical integration of some field data[6] at the exit of the Quadrant II region for the last 12 degrees of the quadrant and into the straight section gives a shortage of flux equal to about 0.47 inches of a sector. This raises a question as to what is the correct value. The effect of this correction will be discussed later, when the energy evaluation is made. There is a gap-mounted target at the center of Quadrant III, and a single-point quadrant measurement is planned to check the displacement at intermediate fields.

I have a computer program to calculate closed orbits by summing values over a number of turns around the Bevatron for a small betatron oscillation and printing out average values at a number of orbit positions. Both the sector perturbations and the quadrant-end effects can be put in. It gives the same values for closed-orbit calculations for sector perturbations as the harmonic analysis. The results for quadrant-end effects agree with the above half-sector calculation. The computer program is also easier to use, particularly for nonsymmetric effects.

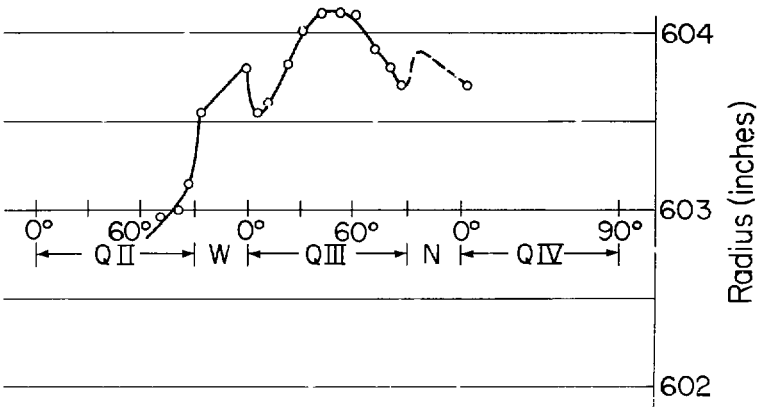

XBL 824-436

Fig. 6. Measured closed orbit through Quadrant III.

A small change in the quadrant-end perturbation in the North compared to the other straight sections provides a reasonable fit to the measured closed orbit at 600 MeV/amu. It is not an unreasonable assumption, as the presence of substantial iron in the extra concrete shielding on top of the north tangent tank could easily cause a small change in the fringe-field flux in this area. Overhead cranes increase the field in the sectors underneath by about 5 gauss at high fields. The effect appears to be caused by the extra iron in the fringe-field flux above the magnet.[7]

One additional potential source of field asymmetry is from the modified leg slabs at the exits of Quadrants II and III. The leg slab reluctance was maintained the same as the standard leg slabs. I am not aware of any measurements to check the variations in the quadrant length. The original leg slabs are being reinstalled prior to the uranium-beam modifications. This may cause some changes in the closed orbit, and measurements will have to be made. The corrections to the path length measurement required by these quadrant length variations will be discussed in Section III.

III. PARTICLE ENERGY

A. Time-of-Flight Measurement

The variations of magnetic field on a sector-by-sector basis, as well as the large quadrant-end effect, make it very difficult to provide a precise evaluation of the particle energy from a known radial position and the value of the magnetic field in the Bevatron. However, for heavy ions it is possible to make a time-of-flight measurement within the Bevatron to provide a more precise value for the particle energy. We must now determine how well we need

to know the path length and transit time to establish a better energy measurement.

As we are working with particles in the relativistic region, we must determine the relationship between changes in kinetic energy and changes in β. We can derive the relationship as follows:

$$E = E_0 (1-\beta^2)^{-1/2} ,$$

$$E = E_0 + KE .$$

where: E = total energy,

E_0 = rest energy,

KE = kinetic energy.

Substituting and solving for KE gives:

$$KE = E_0 \left[(1-\beta^2)^{1/2} - 1\right] . \tag{3-1}$$

Taking the derivative of Eq. (3-1) and dividing by KE gives:

$$\frac{dKE}{KE} = \frac{\beta^2}{(1-\beta^2) - (1-\beta^2)3/2} \frac{d\beta}{\beta} . \tag{3-2}$$

Substituting $\beta = \left[1-(E_0/E)^2\right]^{1/2}$, we have:

$$\frac{dKE}{KE} = \left[\left(\frac{KE}{E_0}\right)^2 + \frac{3KE}{E_0} + 2\right] \frac{d\beta}{\beta} . \tag{3-3}$$

For a time-of-flight measurement in the Bevatron, the velocity is given by:

$$v = sf , \tag{3-4}$$

where: f = frequency on the accelerating electrode,

s = equivalent path length.

The error in v for errors in s and f is given by:

$$\frac{\Delta v}{v} = \left[\left(\frac{\Delta s}{s}\right)^2 + \left(\frac{\Delta f^2}{f}\right)\right]^{1/2} .$$

The frequency is measured with an HP-5360A frequency counter to 1 part in 10^6 for the measurements routinely made. By increasing the measurement time, it can read to 1 part in 10^{10}. Therefore we have:

$$\frac{\Delta v}{v} \approx \frac{\Delta s}{s} . \tag{3-5}$$

The error in the velocity is essentially determined by the error in the path length. The path length in the Bevatron is given by:

$$S = 2\pi R_0 + 4L , \tag{3-6}$$

where: R_0 *is the mean value of the closed orbit; and*

L is the length of each straight section.

The error in S is given by:

$$\frac{ds}{s} = \frac{dR_0}{R_0 + 4L/2\pi} . \tag{3-7}$$

The error in v is therefore:

$$\frac{dv}{v} = \frac{dR_0}{R_0 + 4L/2\pi} . \tag{3-8}$$

To determine how well we must know the closed orbit dR_0 for an energy variation of 0.5%, we proceed as follows. From Eq. (3-3) for a value of 500 MeV/amu, we have:

$$\frac{dKE}{KE} = 3.90 \frac{d\beta}{\beta} , \tag{3-9}$$

$$\frac{dv}{v} = \frac{d\beta}{\beta} = 0.256 \frac{dKE}{KE} ,$$

$$\frac{dv}{v} = 0.256 \times 0.005 ,$$

$$\frac{dv}{v} = 1.28 \times 10^{-3} .$$

Substituting in Eq. (3-8) yields:

$$dR_0 = \left(R_0 + \frac{4L}{2\pi}\right) 1.28 \times 10^{-3}$$

$$= \left(604 + \frac{4 \times 20 \times 12}{2\pi}\right) 1.28 \times 10^{-3} ,$$

$$dR_0 = 0.97 \text{ inches} .$$

Therefore, if we measure R_0 to 0.5 inches, we can determine the KE to 0.25% at 500 MeV/amu.

B. Path Length Correction for Scalloped Orbit from Quadrant Length Correction

We can calculate the path length correction for the scalloped orbit as follows. As the radial beam positions are measured at the straight sections, we can take the closed orbit radius R_0 as going through position A(2) in Fig. 5. We want to calculate the difference in path length between the scalloped orbit and the straight orbit R_0. From Eqs. (2-2) and (2-6) we have:

$$dl \approx Rd\theta = [R_e + A \sin(\nu\theta + D)] d\theta ,$$

$$L = \int_0 \left[R_e \frac{\pi}{4} + A \sin(\nu\theta + D)\right] d\theta \quad ,$$

$$L = R_e \frac{\pi}{4} + \frac{A}{\nu} \cos(\nu\theta + D) \frac{\pi}{4} \quad ,$$

where:

$$A = A_1 \quad , \quad D = \frac{3\pi}{2} \quad , \quad \nu = 0.576 \quad ,$$

$$L = R_e \frac{\pi}{4} - \frac{3.97}{0.576} DL \left[0.4371-0\right] \quad , \tag{3-10}$$

$$L = R_e \frac{\pi}{4} - 3.013\ DL \quad .$$

The path length difference between the circular orbit and the above path length for one-half of a quadrant is given by:

$$\Delta L = R_o \frac{\pi}{4} - L \quad .$$

By substituting Eqs. (2-7) and (3-10) in the above for $R_e = R_o + A_2$, we have the path length difference in half a quadrant:

$$\Delta L = 0.209\ DL \quad .$$

The fractional path length change, including the straight section, is:

$$\frac{\Delta C}{C} = \frac{\Delta L}{2\pi R_o/8+10\times 12} \quad . \tag{3-11}$$

For R_o = 604 inches we have:

$$\frac{\Delta C}{C} = -3.51 \times 10^{-4}\ DL \quad . \tag{3-12}$$

This is the path length correction for the scalloped orbit relative to the measured closed orbit at the straight sections through the radius R_o.

C. Correction to Measured Radial Position for Fringe-Field Effect

The probes used to measure the radial position of the beam are in the field-free regions of the straight sections. The particle energy is determined by the radial position in the quadrants. A correction must therefore be made for the outward radial drift of the orbit when passing through the fringe field.

A plot of the calculated orbit, using the fringe-field data of MT-87 for the Quadrant II exit, is shown in Fig. 7. The measured value was about 0.25 inches using the travel target in Quadrants II and III. This agrees with the calculation in Fig. 7.

D. Errors in Kinetic Energy Measurement

In Section III-B, we determined that the error in Bevatron time-of-flight measurements is essentially from the error in the path length. I will now evaluate the error in the kinetic energy measurement as a result of the errors in the radius measurements and the uncertainty in the closed orbit distortion as a result of the variation in quadrant length of the magnetic field.

The radial position of the circulating particle beam is measured with radial clipper probes in the four straight sections. In the South, West, and North straight sections, these are vertical bars of aluminum 1 inch thick in the azimuthal direction, 1/8 inch thick in the radial direction and 8 inches in the vertical. The North and West clippers are flipped up from below in about 100 msec. The clipper on the south probe is plunged radially outward from the inner radius in about 200 ms.

The East probe is a U-shaped target or harp and is used in two modes. The first mode is to flip the harp up with the beam positioned near the center of the U (Fig. 8). The radial position of the harp is adjusted for maximum

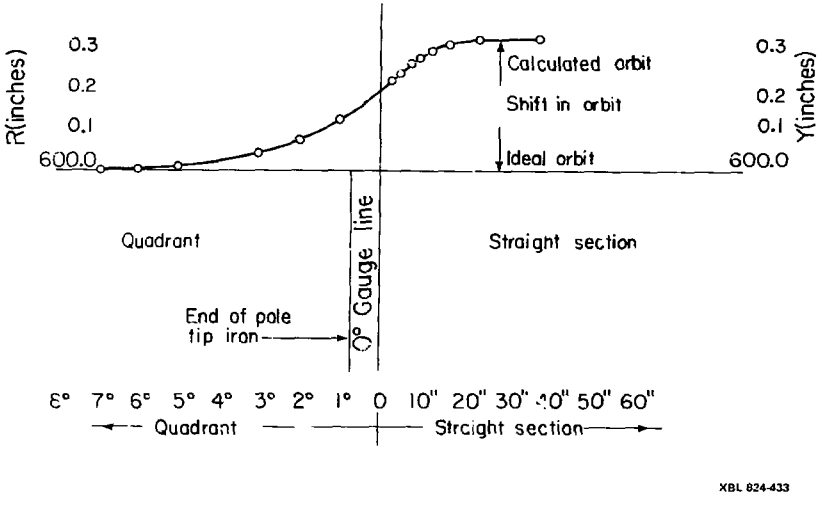

Fig. 7. Fringe-field orbit trajectory.

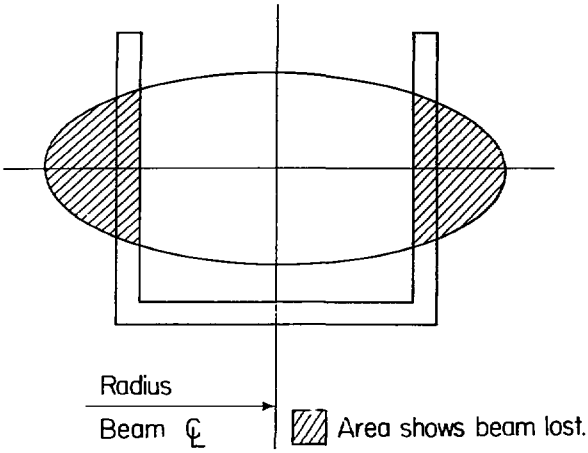

XBL 824-440

Fig. 8. Beam clipping with harp. Shadowed areas show portions of beam that are lost.

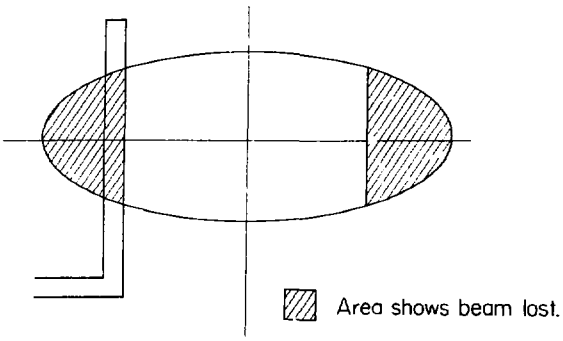

XBL 824-439

Fig. 9. Beam clipping with finger target. Shadowed areas show lost portions of beam.

beam survival. The radial centerline position of the harp is then the radial position of the center of the circulating beam at that probe.

The second mode is used to measure the relative radial position. The U probe is moved radially inward so that it clips the beam on the inside radius only (Fig. 9). The results of these measurements can then be compared to the other three probes, which are finger probes. By comparing the radial probe position for the same beam survival, relative radial beam positions are determined.

The charge of the circulating beam is measured by a capacitive pick-up system called the Beam Induction Electrode (BIE). The BIE value is read just before and just after flipping the probe into the beam. In recent measurements, a voltmeter read the two values and then provided a signal that was the ratio of the two BIE levels. This signal was set to read 1.000 for no probe in the beam. For each Bevatron pulse, the value was printed out on a paper tape. The MODCOMP computer was set up to give a pulse-by-pulse read-out of the magnetic field value and rf frequency for the pulses and this read-out was then printed as a hard copy. The BIE ratio and field and frequency hard copies were manually synchronized during data taking. Runs were made by radially scanning with the probes in 0.2-inch steps for 5 to 6 steps. Data for the finger-probe scans at each straight section are shown in Fig. 10. This gives the relative beam location at each section. Figure 11 shows date for the harp scans with the East probe for the radial position measurement.

From Fig. 10, we can determine the relative radial positions to about ±1/16 inch and the closed orbit radius in the east to ±1/8 inch. The shaft end play on the probes and the absolute radial position calibration are both about ± 1/16 inch. From Section II-A we have an estimate of about 0.16 inches

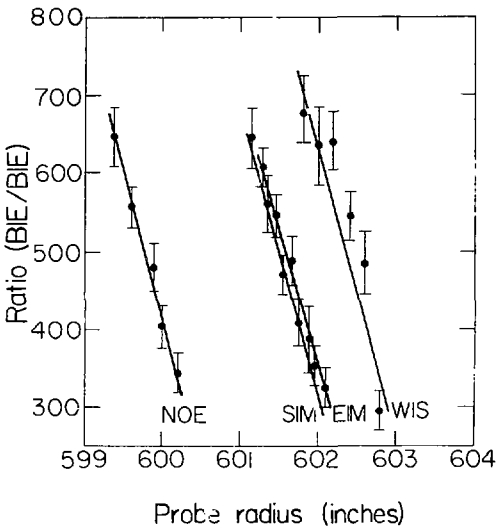

XBL 824-431

Fig. 10. Scan with finger probes; B_0 = 5315 gauss.

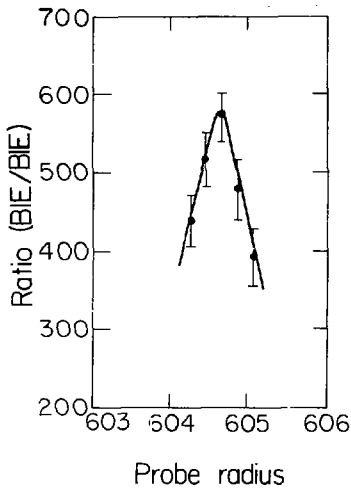

XBL 824-430

Fig. 11. Scan with harp; B_0 = 5315 gauss.

for a possible undetected fourth harmonic. This, then, gives an error in R of:

$$\Delta R = \pm \left[(0.062)^2 + (0.125)^2 + (0.062)^2 + 0.062)^2 + (0.16)^2\right]^{1/2}$$

$$\Delta R = \pm 0.24 \text{ inches} \quad .$$

From Eq. (2-3),

$$R_o = \frac{1}{n} \sum_{j=1}^{m} R(j) \quad ,$$

$$R_o = \frac{1}{4} (R_e + R_s + R_w + R_n) \quad ,$$

$$\left(\frac{\Delta R}{R}\right)_{rms} = \frac{1}{4} \left[\left(\frac{\Delta R_e}{R}\right)^2 + \left(\frac{\Delta R_s}{R}\right)^2 + \left(\frac{\Delta R_w}{R}\right)^2 + \left(\frac{\Delta R_n}{R}\right)^2\right]^{1/2} \quad ,$$

$$= \frac{1}{4} \left[\left(\frac{\Delta R}{R}\right)^2 4\right]^{1/2}$$

$$= \frac{\Delta R}{2R} = \pm \frac{0.24}{2 \times 604} \quad ,$$

$$\left(\frac{\Delta R}{R}\right)_{rms} = \pm 2.02 \times 10^{-4} \quad .$$

The path length error is given from Eq. (3-7):

$$\frac{d_s}{s} = \frac{dR_o}{R_o + \frac{4L}{2\pi}} = \frac{dR_o}{R_o} \frac{1}{1 + \frac{4L}{2\pi} R_o}$$

$$= 0.798 \times \frac{dR_o}{R_o} \quad ,$$

$$\frac{d_s}{s} = \pm 1.61 \times 10^{-4} \quad .$$

The path length correction for a scalloped orbit from the quadrant length correction was given by Eq. (3-12):

$$\frac{\Delta C}{C} = \pm 3.51 \times 10^{-4} \text{ DL} \quad .$$

At the region of maximum correction, if the error in the quadrant length correction was a factor of 2, the error in DL would be 1.5 inches. The error in path length would then be:

$$\frac{\Delta C}{C} = \pm 3.51 \times 10^{-4} \times 1.5$$

$$= \pm 5.27 \times 10^{-4} \quad .$$

The error in the path length for this correction and the error in R_0 is given by:

$$\left(\frac{\Delta C}{C}\right)_{rms} = \pm \left[(5.27\times10^{-4})^2 + (1.61\times10^{-4})^2\right]^{1/2}$$

$$= \pm 5.27 \times 10^{-4} \quad .$$

From Eq. (3-9), we have for 500 MeV/amu particles:

$$\left(\frac{\Delta KE}{KE}\right)_{rms} = 3.90 \times \frac{d\beta}{\beta} = 3.90 \frac{\Delta S}{S}$$

$$= \pm 3.90 \times 5.51 \times 10^{-4} \quad ,$$

$$\left(\frac{\Delta KE}{KE}\right)_{rms} = \pm 2.15 \times 10^{-3} \quad .$$

That is, we know the kinetic energy to about ±0.25% with the above errors.

If we double the error in R_0 we increase $\Delta KE/KE$ to 2.41×10^{-3}. We can see that the major error is from the uncertainty in the value for the quadrant length correction.

The value of $\Delta KE/KE$ for various values of KE are tabulated in Table 2 for the above values of error, taking the error in DL as one-half of the value tabulated in Table 1.

E. Calculation for Time-of-Flight Measurement

The radius of the closed orbit is determined from the radial probe measurements, as discussed in Section III-D. From Eq. (2-3) in Section I, we have:

$$R_o = \frac{1}{4}\left[R_E + R_S + R_W + R_n\right] .$$

From orbit eccentricity measurements we have:

$$R_S = R_E + \Delta R_S ,$$

$$R_W = R_E + \Delta R_W ,$$

$$R_N = R_E + \Delta R_N .$$

Substituting in the above equation and subtracting 0.25 inches for the fringe-field correction (Section III-C) yields:

$$R_o = R_E + \frac{\Delta R_S}{4} + \frac{\Delta R_W}{4} + \frac{\Delta R_N}{4} - \frac{1}{4} . \qquad (3\text{-}13)$$

The path length is given by:

$$S = 2\pi R_o + 4L . \qquad (3\text{-}14)$$

The correction to the path length for the quadrant length correction from Eq. (3-12) is:

$$\frac{\Delta C}{C} = -3.51 \times 10^{-4}\ DL .$$

Table 2. $\Delta KE/KE$ vs. B_0 for a factor of 2 uncertainty in quadrant length correction for time-of-flight measurement in the Bevatron.

B_0 (kG)	KE (MeV)	$\Delta KE/KE$ (%)
1	28	0.13
2	106	0.16
3	225	0.19
4	373	0.23
5	543	0.27
6	726	0.31
7	920	0.33
8	1120	0.30
9	1327	0.23
10	1537	0.21
11	1750	0.20
12	1965	0.21
13	2182	0.25
14	2401	0.28
15	2621	0.30

Therefore, we have:

$$S = 2\pi R_0 + 4L - 3.51 \times 10^{-4}\ DL\ (2\pi R_0 + 4L) \quad ,$$

$$S = (2\pi R_0 + 4L)\ (1-3.51 \times 10^{-4}\ DL) \quad . \tag{3-15}$$

β is given by:

$$\beta = \frac{Sf}{C} \quad ,$$

where: f = measured frequency of rotation,

C = velocity of light,

$$\beta = \frac{f}{C}\ [2\pi R_0 + 4L]\ [1-3.51 \times 10^{-4}\ DL] \quad . \tag{3-16}$$

From Eq. (3-1) we have for the kinetic energy of the particle:

$$KE = E_0\ [(1-\beta^2)^{-1/2} - 1] \quad . \tag{3-17}$$

To determine the particle energy in the Bevatron, proceed as follows. If the orbit eccentricities are known from previous measurements (ΔR_S; ΔR_W; ΔR_N), then only the radial position in the east and the frequency of the rf system are needed. Equation (3-13) gives R_0 from the radial position measurements. DL is given in Table 1. Substituting in Eqs. (3-16) and (3-17) gives the value for KE. The typical values for $\Delta KE/KE$ as a function of KE are given in Table 2.

REFERENCES

1. K.C. Crebbin, "Bevatron Parameters," Bev-3187, January 9, 1976.

2. L.G. Ratner, "Bevatron Magnet--Magnetic Field Measurements," UCID-599, MT-87, September 24, 1958.

3. "I-Pip Time, Current, Flux, Frequency, and Energy Chart," Lawrence Berkeley Laboratory Engineering Print 9Y7083A, January 9, 1964.

4. D.J. Rondeau, "Main Guide Field Calibration," Memorandum, June 24, 1975.

5. K.C. Crebbin and G.R. Lambertson, "Magnet Alignment," Bev-974, December 20, 1967.

6. P.G. Watson, "Flux Density in West Target Area for Magnet Currents 4001, 7001, and 8334 Amperes," MT-29, August 12, 1955.

7. R.W. Brokloff and K.C. Crebbin, "Bevatron Operation and Development," no. 50, UCRL-17223, TID-4500 (49th Ed.), November 17, 1966.

APPENDIX

The following derivation calculates the closed orbit in terms of a summation of simple betatron oscillations, based on the assumption that the Bevatron is composed of a perfect machine plus 144 perturbations, one at each sector.

From Fig. 3 for $\theta > \theta_j$ we have:

$$\theta_p = \theta_j + \pi - \theta \quad .$$

The displacement $R\theta$ at θ_p from a perturbation at θ_j is:

$$R\theta = A_j \sin\left(\frac{3\pi}{2} - \nu\theta_p\right)$$

$$= A_j \left(\sin\frac{3\pi}{2} \cos \nu\theta_p - \cos\frac{3\pi}{2} \sin \nu\theta_p\right) \quad ,$$

$$R\theta = -A_j \cos \nu\theta_p$$

$$= -A_j \cos \nu(\theta_j + \pi - \theta)$$

$$R\theta = -A_j \cos\left[\nu\pi - \nu(\theta-\theta_j)\right] \quad . \tag{A-1}$$

From Fig. 4 for $\theta < \theta_j$ we have:

$$\theta_p = \pi - (\theta_j - \theta) \quad ,$$

$$R\theta = A_j \sin\left(\frac{3\pi}{2} + \nu\theta_p\right) \quad .$$

By expansion as above we have:

$$R\theta = -A_j \cos\left[\nu\pi - \nu(\theta_j - \theta)\right] \quad . \tag{A-2}$$

For the ith position, where $\theta = \theta_i$, the displacement R_i is the sum over j of all the individual displacements:

$$R_i = \sum_{j=1}^{i} A_j \cos\left[\nu\pi - \nu(\theta_j - \theta_i)\right] - \sum_{j=i+1}^{144} A_j \cos\left[\nu\pi - \nu(\theta_i - \theta_j)\right] .$$

Separating out the θ_i term gives:

$$R_i = -\sum_{j=1}^{i} A_j \cos\left[(\nu\pi - \nu\theta_j) + \nu\theta_i\right] - \sum_{j=i+1}^{144} A_j \cos\left[(\nu\pi + \nu\theta_j) - \nu\theta_i\right] .$$

Expanding gives:

$$R_i = -\sum_{j=1}^{i} A_j \left[\cos \nu(\pi - \theta_j) \cos \nu\theta_i - \sin \nu(\pi - \theta_j) \sin \nu\theta_i\right]$$

$$- \sum_{j=i+1}^{144} A_j \left[\cos \nu(\pi + \theta_j) \cos \nu\theta_i + \sin \nu(\pi + \theta_j) \sin \nu\theta_i\right] .$$

Factoring gives:

$$R_i = -\cos \nu\theta_i \left[\sum_{j=1}^{i} A_j \cos \nu(\pi - \theta_j) + \sum_{j=i+1}^{144} A_j \cos \nu(\pi + \theta_j)\right]$$

$$+ \sin \nu\theta_i \left[\sum_{j=1}^{i} A_j \sin \nu(\pi - \theta_j) - \sum_{j=i+1}^{144} A_j \sin \nu(\pi + \theta_j)\right] .$$

Expanding again gives:

$$R_i = -\cos\nu\theta_i \left[\sum_{j=1}^{i} A_j \left(\cos\nu\pi \cos\nu\theta_j + \sin\nu\pi \sin\nu\theta_j\right) + \sum_{j=1+1}^{144} A_j \left(\cos\nu\pi \cos\nu\theta_j - \sin\nu\pi \sin\nu\theta_j\right) \right]$$

$$+ \sin\nu\theta_i \left[\sum_{j=1}^{i} A_j \left(\sin\nu\pi \cos\nu\theta_j - \cos\nu\pi \sin\nu\theta_j\right) - \sum_{j=i+1}^{144} A_j \left(\sin\nu\pi \cos\nu\theta_j + \cos\nu\pi \sin\nu\theta_j\right) \right] .$$

Factoring yields:

$$R_i = -\cos\nu\theta_i \left[\cos\nu\pi \sum_{j=1}^{i} A_j \cos\nu\theta_j + \sin\nu\pi \sum_{j=1}^{i} A_j \sin\nu\theta_j \quad \cos\nu\pi \sum_{j=i+1}^{144} A_j \cos\nu\theta_j - \sin\nu\pi \sum_{j=i+1}^{144} A_j \sin\nu\theta_j \right]$$

$$+ \sin\nu\theta_i \left[\sin\nu\pi \sum_{j=1}^{i} A_j \cos\nu\theta_j - \cos\nu\pi \sum_{j=1}^{i} A_j \sin\nu\theta_j \quad - \sin\nu\pi \sum_{j=i+1}^{144} A_j \cos\nu\theta_j - \cos\nu\pi \sum_{j=i+1}^{144} A_j \sin\nu\theta_j \right] .$$

Collecting terms:

$$R_i = -\cos\nu\theta_i \left[\cos\nu\pi \sum_{j=1}^{i} A_j \cos\nu\theta_j + \sin\nu\pi\left(\sum_{j=1}^{i} A_j \sin\nu\theta_j - \sum_{j=i+1}^{144} A_j \sin\nu\theta_j\right)\right]$$

$$+ \sin\nu\theta_i \left[\sin\nu\pi\left(\sum_{j=1}^{i} A_j \cos\nu\theta_j - \sum_{j=1}^{144} A_j \cos\nu\theta_j\right) - \cos\nu\pi \sum_{i=1}^{144} A_j \cos\nu\theta_j\right] .$$

This can be rewritten:

$$R_i = -\cos\nu\theta_i \left[\cos\nu\pi\, S_1 + \sin\nu\pi\left(\sum_{j=1}^{i} A_j \sin\nu\theta_j - \sum_{j=i+1}^{144} A_j \sin\nu\theta_j\right)\right]$$

$$+ \sin\nu\theta_i \left[\sin\nu\pi\left(\sum_{j=1}^{i} A_j \cos\nu\theta_j - \sum_{j=i+1}^{144} A_j \cos\nu\theta_j - \cos\nu\pi\, S_2\right)\right] , \qquad \text{(A-3)}$$

where:

$$S_1 = \sum_{j=1}^{144} A_j \cos\nu\theta_j ,$$

$$S_2 = \sum_{j=1}^{144} A_j \sin\nu\theta_j .$$

Equation (A-3) can be written in the form:

$$R_i = B(i) \cos\nu\theta_i + D(i) \sin\nu\theta_i , \qquad \text{(A-4)}$$

where:

$$B(i) = -\sin\nu\pi\left(\sum_{j=1}^{i} A_j \sin\nu\theta_j - \sum_{j=i+1}^{144} A_j \sin\nu\theta_j\right) - S_1 \cos\nu\pi \quad ,$$

$$D(i) = \sin\nu\pi\left(\sum_{j=1}^{i} A_j \cos\nu\theta_j - \sum_{j=1}^{144} A_j \cos\nu\theta_j\right) - S_2 \cos\nu\pi \quad .$$

Equation (A-4) can be put in the form:

$$R_i = H(i) \cos\left(\nu\theta_i + \delta(i)\right) \quad . \tag{A-5}$$

Equation (A-5) is a first harmonic betatron oscillation with slowly varying amplitude and phase to provide a closed orbit.

To examine the change in R between R_i and R_{i+1}, we can use Eq. (A-4):

$$R_{i+1} - R_i = B(i+1) \cos\nu\theta_{i+1} + D(i+1) \sin\nu\theta_{i+1} - B(i) \cos\nu\theta_i - D(i) \sin\nu\theta_i \quad . \tag{A-6}$$

B(i+1) is given by:

$$B(i+1) = -\sin\nu\pi\left(\sum_{j=1}^{i+1} A_j \sin\nu\theta_j - \sum_{j=1+2}^{144} A_j \sin\nu\theta_j\right) - S_1 \cos\nu\pi \quad .$$

Factoring out the A_i term yields:

$$B(i+1) = -\sin\nu\pi\left(\sum_{j=1}^{i-1} A_j \sin\nu\theta_j + A_i \sin\nu\theta_i + A_{i+1} \sin\nu\theta_{i+1} - \sum_{j=1}^{144} A_j \sin\nu\theta_j + A_i \sin\nu\theta_i + A_{i+1} \sin\nu\theta_{i+1}\right) - S_1 \cos\nu\pi \quad .$$

Collecting terms:

$$B(i+1) = -\sin\nu\pi\left(\sum_{j=1}^{i-1} A_j \sin\nu\theta_j - \sum_{j=1}^{144} A_j \sin\nu\theta_j\right) - S_1 \cos\nu\pi$$

$$-\sin\nu\pi\left(2A_i \sin\nu\theta_i + 2\, A_{i+1} \sin\nu\theta_{i+1}\right) ,$$

$$B(i+1) = B(i-1) - \sin\nu\pi\left(2A_i \sin\nu\theta_i + 2\, A_{i+1} \sin\nu\theta_{i+1}\right) . \qquad \text{(A-7)}$$

Similarly for the D(i+1) term:

$$D(i+1) = \sin\nu\pi\left(\sum_{j=1}^{i+1} A_j \cos\nu\theta_j - \sum_{j=1+2}^{144} A_j \cos\nu\theta_j\right) - S_2 \cos\nu\pi .$$

Factoring out the A_i term:

$$D(i+1) = \sin\nu\pi\left(\sum_{j=1}^{i=1} A_j \cos\nu\theta_j + A_i \cos\nu\theta_i + A_{i+1} \cos\nu\theta_{i+1}\right.$$

$$\left. - \sum_{j=1}^{144} A_j \cos\nu\theta_j + A_i \cos\nu\theta_i + A_{i+1} \cos\nu\theta_{i+1}\right)$$

$$- S_2 \cos\nu\pi .$$

Collecting terms:

$$D(i+1) = \sin\nu\pi\left(\sum_{j=1}^{i-1} A_j \cos\nu\theta_j - \sum_{j=1}^{144} A_j \cos\nu\theta_j\right) - S_2 \cos\nu\pi$$

$$+ \sin\nu\pi\left(2A_i \cos\nu\theta_i + 2A_{i+1} \cos\nu\theta_{i+1}\right) ,$$

$$D(i+1) = D(i-1) + \sin\nu\pi\left(2A_i \cos\nu\theta_i + 2A_{i+1} \cos\nu\theta_{i+1}\right) . \qquad \text{(A-8)}$$

B(i) is given by:

$$B(i) = -\sin\nu\pi\left(\sum_{j=1}^{i} A_j \sin\nu\theta_j - \sum_{j=i+1}^{144} A_j \sin\nu\theta_j\right) - S_1 \cos\nu\pi \quad .$$

Factoring out the A_i term:

$$B(i) = -\sin\nu\pi\left(\sum_{j=1}^{i-1} A_j \sin\nu\theta_j + A_i \sin\nu\theta_i - \sum_{j=i}^{144} A_j \sin\nu\theta_j + A_i \sin\nu\theta_i\right) - S_1 \cos\nu\pi$$

$$= -\sin\nu\pi\left(\sum_{j=1}^{i-1} A_j \sin\nu\theta_j - \sum_{j=1}^{144} A_j \sin\nu\theta_j\right) - S_1 \cos\nu\pi - 2 \sin\nu\pi\, A_i \sin\nu\pi \quad ,$$

$$B(i) = B(i-1) - 2 A_i \sin\nu\theta_i \sin\nu\pi \quad . \qquad \text{(A-9)}$$

Similarly for the D(i) term:

$$D(i) = -\sin\nu\pi\left(\sum_{j=1}^{i} A_j \cos\nu\theta_j - \sum_{j=i+1}^{144} A_j \cos\nu\theta_j\right) - S_2 \cos\nu\pi \quad .$$

Factoring out the A_i term:

$$D(i) = \sin\nu\pi\left(\sum_{j=1}^{i-1} A_j \cos\nu\theta_j + A_i \cos\nu\theta_i - \sum_{j=i}^{144} A_j \cos\nu\theta_j + A_i \cos\nu\theta_i\right) - S_2 \cos\nu\pi \quad ,$$

$$D(i) = \sin\nu\pi\left(\sum_{j=1}^{i-1} A_j \cos\nu\theta_j - \sum_{j=1}^{144} A_j \cos\nu\theta_j\right) - S_2 \cos\nu\pi + 2\, A_i \cos\nu\theta_i \sin\nu\pi$$

$$= D(i-1) + 2\, A_i \cos\nu\theta_i \sin\nu\pi \quad . \qquad \text{(A-10)}$$

Substituting (A-7), (A-8), (A-9), and (A-10) in Eq. (A-6) gives:

$$\begin{aligned} R_{i+1} - R_1 = {} & \{B(i-1) - \sin\nu\pi\,[2A_i \sin\nu\theta_i + 2A_{i+1} \sin\nu\theta_{i+1}]\} \cos\nu\theta_{i+1} \\ & + \{D(i-1) + \sin\nu\pi\,[2A_i \cos\nu\theta_i + 2A_{i+1} \cos\nu\theta_{i+1}]\} \sin\nu\theta_{i+1} \\ & - \{B(i-1) - \sin\nu\pi\, 2A_i \sin\nu\theta_i\} \cos\nu\theta_i \\ & - \{D(i-1) + \sin\nu\pi\, 2A_i \cos\nu\theta_i\} \sin\nu\theta_i \quad . \end{aligned}$$

Collecting terms yields:

$$\begin{aligned} R_{i+1} - R_i = {} & B(i-1)\,(\cos\nu\theta_{i+1} - \cos\nu\theta_i) + D(i-1)\,(\sin\nu\theta_{i+1} - \sin\nu\theta_i) \\ & - \sin\nu\pi\,[2A_i \sin\nu\theta_i \cos\nu\theta_{i+1} + 2A_{i+1} \sin\nu\theta_{i+1} \cos\nu\theta_{i+1} \\ & - 2A_i \cos\nu\theta_i \sin\nu\theta_{i+1} - 2A_{i+1} \cos\nu\theta_{i+1} \sin\nu\theta_{i+1} \\ & - 2A_i \sin\nu\theta_i \cos\nu\theta_i + 2A_i \cos\nu\theta_i \sin\nu\theta_i] \quad , \end{aligned}$$

$$\begin{aligned} R_{i+1} - R_i = {} & B(i-1)\,[\cos\nu\theta_{i+1} - \cos\nu\theta_i] + D(i-1)[\sin\nu\theta_{i+1} - \sin\nu\theta_i] \\ & - \sin\nu\pi\, 2A_i\,[\sin\nu\theta_i \cos\nu\theta_{i+1} - \cos\nu\theta_i \sin\nu\theta_{i+1}] \quad . \end{aligned}$$

Substituting $\theta_{i+1} = \theta_1 + \Delta\theta$ gives:

$$R_{i+1} - R_i = B(i-1)\left[\cos(\nu\theta_i + \nu\Delta\theta) - \cos\nu\theta_i\right]$$
$$+ D(i-1)\left[\sin(\nu\theta_i + \nu\Delta\theta) - \sin\nu\theta_i\right]$$
$$- 2A_i \sin\nu\pi \left[\sin\nu\theta_i \cos(\nu\theta_i + \nu\Delta\theta) - \cos\nu\theta_i \sin(\nu\theta_i + \nu\Delta\theta\right] .$$

Expanding:

$$R_{i+1} - R_i = B(i-1)\left[\cos\nu\theta_i \cos\nu\Delta\theta - \sin\nu\theta_i \sin\nu\Delta\theta - \cos\nu\theta_i\right]$$
$$+ D(i-1)\left[\sin\nu\theta_i \cos\nu\Delta\theta + \cos\nu\theta_i \sin\nu\Delta\theta - \sin\nu\theta_i\right]$$
$$- 2A_i \sin\nu\pi \left[\sin\nu\theta_i (\cos\nu\theta_i \cos\nu\Delta\theta - \sin\nu\theta_i \sin\nu\Delta\theta)\right.$$
$$\left. - \cos\nu\theta_i (\sin\nu\theta_i \cos\nu\Delta\theta + \cos\nu\theta_i \sin\nu\Delta\theta)\right] ,$$

$$R_{i+1} - R_i = B(i-1)\left[\cos\nu\theta_i - \sin\nu\theta_i\ \nu\Delta\theta - \cos\nu\theta_i\right]$$
$$+ D(i-1)\left[\sin\nu\theta_i + \cos\nu\theta_i\ \nu\Delta\theta - \sin\nu\theta_i\right]$$
$$- 2A_i \sin\nu\pi \left[\sin\nu\theta_i \cos\nu\theta_i - \sin^2 \nu\theta_i\ \nu\Delta\theta\right.$$
$$\left. - \cos\nu\theta_i \sin\nu\theta_i - \cos^2 \nu\theta_i\ \nu\Delta\theta\right] ,$$

$$R_{i+1} - R_i = -B(i-1) \sin\nu\theta_i\ \nu\Delta\theta + D(i-1) \cos\nu\theta_i\ \nu\Delta\theta$$
$$+ 2A_i \sin\nu\pi \left[\sin^2\nu\theta_i + \cos^2\nu\theta_i\right] \nu\Delta\theta ,$$

$$R_{i+1} - R_i = -B(i-1) \sin\nu\theta_i\ \nu\Delta\theta + D(i-1) \cos\nu\theta_i\ \nu\Delta\theta$$
$$+ 2A_i \sin\nu\pi\ \nu\Delta\theta . \qquad \text{(A-11)}$$

The first two terms of Eq. (A-11) are the derivative of Eq. (A-4) with constant coefficients B and D evaluated at i-1. The third term is the contribution from the changing coefficients and is just equal to twice the derivative of the ith perturbed orbit at the ith position (see Fig. A-1).

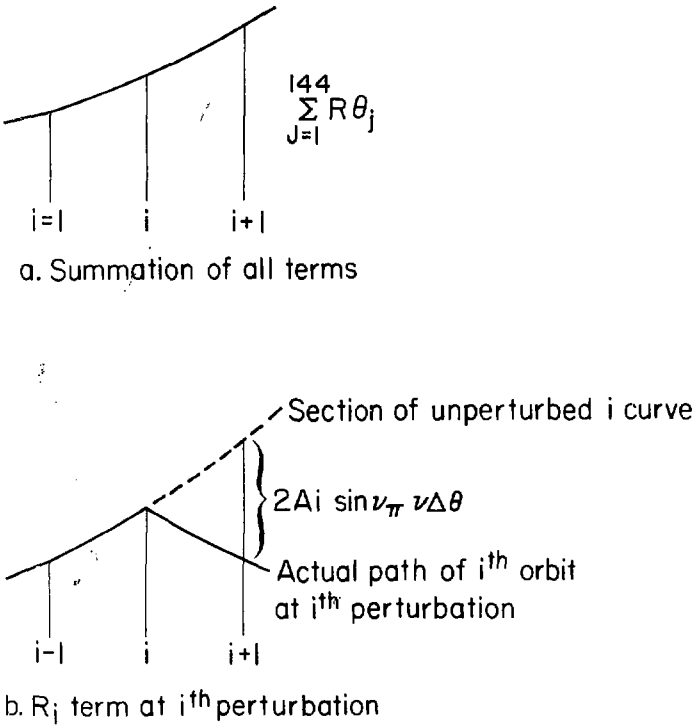

XBL 824-432

Fig. A-1. Closed orbit at ith sector with and without perturbation.

(a) Summation of all terms;

(b) actual path of ith orbit at ith perturbation.